NuMI-B-933
Version 0.0

DESIGN OF THE PROTOTYPE NUMI PROFILE MONITOR SEM

Sacha E. Kopp, Marek Proga
Dept. of Physics, University of Texas, Austin, Texas

ABSTRACT

The NuMI primary proton beam profile will be monitored by a series of secondary emission monitors (SEM's). The present note describes the design of a SEM which implements 5μm Ti foils, segmented for *X* and *Y* readout, moving on a sliding "gate-valve"-like frame. The foil-supporting frame remains out of the beam during insertion and removal of the device, permitting insertion without stoppage of the beam. A prototype detector has been assembled for testing in the MiniBoone 8 GeV transfer line.

I. INTRODUCTION

Beam profile may be measured via the process of secondary electron emission [1]. A secondary electron monitor (SEM) consists of a metal screen of low work function from which low (<100 eV) energy electrons are ejected. While the probability for such emission is low (~0.01/beam particle), such monitors produce signals of 10-100nC when 4×10^{13} beam particles per spill pass through the device, permitting their use as beam monitors[2]. Furthermore, the process of secondary electron emission is a surface phenomenon [3,4,5,6], so that electron emitting foils or wires of very thin (1-10 μm) dimensions may be used without penalty to the signal size [7]. Often a positive voltage ("clearing field") is used to draw the secondary electrons cleanly away from the signal screen. A schematic SEM is shown in Figure 1.

Secondary electron emission monitors have replaced ionization chambers as beam monitors for over 40 years [2]. An ionization chamber monitors beam intensity by measuring the ionized charge in a gas volume collected on a chamber electrode. Such a device places large ($\sim10^{-2}$-10^{-3} λ_{int}) amount of material in the beam which results in emittance blowup and beam loss, both of which are unacceptable in high intensity beams. As will be discussed, the prototype SEM discussed in this note is 7×10^{-6} λ_{int} in thickness. A further limitation of ionization chambers is that space charge buildup limits them to measurements of beams with intenstities of $<10^{14}$ particles/cm^2/sec [8], nearly 6 orders of magnitude below the NuMI requirements. SEM's, in contrast, are extremely linear in response [2,9].

For the NuMI beam, we desire a segmented SEM which measures not only beam intensity but also the centroid position and lateral profile. The beam spot is anticipated to be $\sigma\sim$1mm. The required SEM segmentation is of order 1mm. The two SEM's near the NuMI target require segmentation of 0.5mm in order to specify the beam position and angle onto the target at the 50 μrad level. The segmented SEM will measure profile out to 1" radius. A single, large foil will cover the remaining aperture out to 2" radius in order to measure any potential beam halo.

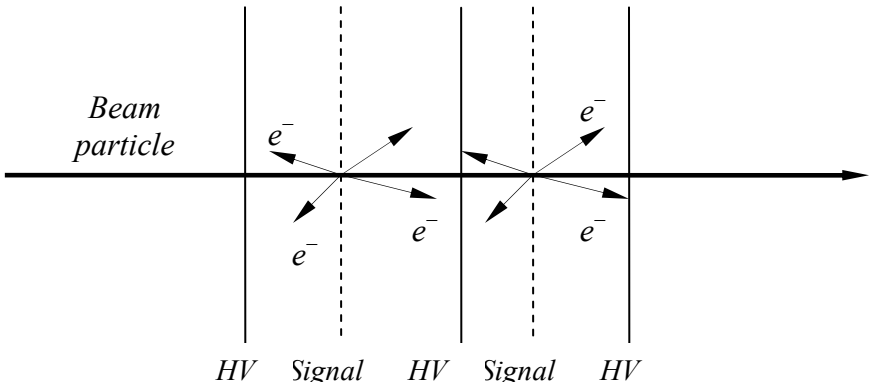

Figure 1: Schematic diagram of a segmented secondary emission monitor. Beam particles pass through an active medium, emitting secondary electrons. These electrons may be drawn away from the signal screen by a voltage ~30-1000V to prevent contamination of adjacent signal screens.

II. PROFILE SEM REQUIREMENTS

Secondary emission monitors have been employed at all major accelerator labs. However, the requirements for NuMI motivate a new design:

1. The device must survive ~10^{20} particles/cm^2 per year.
2. Groundwater activation in the carrier tunnel region requires beam loss ~10^{-6}.
3. The beam centroid position accuracy must be ~50μm.
4. The SEM chamber vacuum must be 10^{-8} Torr.
4. The measurement aperture must be ~2". The clear aperture must be 4".
5. The device must be removable from the beam without turning off the beam.
6. Replacement of the device in the beam must be achieved to 50μm positional accuracy.

The first two requirements pertain mostly to the active medium of the SEM, namely that the secondary emission yield not drop precipitously with integrated beam exposure and that the SEM material in the beam be fairly low mass so as not to cause beam loss. These two factors are discussed in Section III, where we review relevant properties of SEM materials used by others.

The remaining requirements motivate the mechanical design discussed in the rest of this note. We have developed a prototype foil SEM with 1 mm segmentation to provide the required positional accuracy. The design mounts the foils on a paddle that slides in and out of the beam like a gate valve in a vacuum chamber. The paddle wraps around the beam, so is always out of the beam during SEM insertion and removal. The challenges of this design are the large aperture to be maintained and the handling of delicate foils. The prototype developed here demonstrates the feasibility of the mechanical assembly.

For the prototype, we have not automated the mechanism for insertion and removal of the device in the beam. A motorized linear feedthrough is produced by Huntington Vacuum (model L-2250-T) which will be employed for the final design, but for now a manual push-pull version of this feedthrough has been employed. The features that will be demonstrated with this prototype are a design that can withstand long beam exposures, cause low beam loss, uses low-vacuum compatible materials, and maintains the required aperture. As shall be shown, the switch to motorized feedthrough will be readily accomplished.

Material	Z	X_0 (cm)	λ_{int} (cm)	SEE (%)	Propose wire/foil	Thickness (μm)	Beam Loss (10^{-6})	Comments
Be	4	35.3	40.6	?	foil	25	12	SEE unknown; foils <0.001" difficult to procure; biological hazard
C	6	18.8	38.1	2-2.5	Wire	33	2.7	Withstands high temperature; used at LANL, SLAC as wire scanner; fragile.
Al	13	8.9	39.3	~7	Foil	5	2.5	SEE ages badly in beam [11,13]
Ti	22	3.6	27.5	3.5	Foil	5	3.6	Excellent longevity to 10^{20} p/cm^2 dose[13]
Ni	28	1.46	~15[a]	3-5?	Foil	10	13	Ages in beam [16]
Ag	47	0.87	~9[b]	~6	Foil	5	~10	Data from [11], but requires great care because oxidation will degrade signal.
W	74	0.35	9.6	4	Wire	75	60	SEE is for Au-plated wire[15]. Breaks if wire is < 75mm (Gianni Tassotto)
Au	79	0.30	8.8[c]	~7	Foil	10	22	Does not oxidize, but does adsorb CO [11]; signal loss observed [13]

[a]Value for Cu (Z=29,ρ=8.9g/cc) [b]Scaled from λ_{int}(Cu) using $\lambda^{-1} \propto A^{0.77}$[21]
[c]Value for Pt (Z=78,ρ=21.5g/cc)

Table 1: Properties of potential active media to be used in the SEM profile monitor. The estimated beam loss assumes a 1mm beam spot size and, in the case of foil strips, a strip width of 0.2mm.

III. SEM ACTIVE MEDIUM

Previous workers have noted the secondary electron emission (SEE) yield drops for large integrated exposures [10,11,12,13]. For beam nominally on center through a long run, such signal loss results in degraded beam centroid magnitude and also results in artificially enhanced beam tails, since the beam tails irradiate the SEM to a lesser extent. Possible physical causes of the loss of signal have been attributed to modification of the metal's work function by irradiation of hydrocarbon, oxide, or CO layers on the material surface. Such radiaton effects are thought to be accelerated by heating of the surface. Several SEM's have been discussed which were cleaned using glow discharges of the surface to remove layers, but require extremely process intensive treatments and great care never to expose the metal to air. Such processes are impractical on a large scale.

The requirement of low beam loss motivates the choice of low atomic number materials, which typically also have nuclear interaction lengths λ_{int}~30-40 cm. At Fermilab, the most common SEM in use at present is the 'multi-wire', planes of 75 μm Ø Au-plated W(97%)-Rh(3%) wire [14]. Being made of Tungsten, a plane of these wires strung at 1 mm pitch causes beam loss of 60×10^{-6} (see Table 1), which exceeds our requirements unless their time in the beam is limited to <5% of beam live time. Further, the secondary emission of such wires dropped by 20% in KTeV operation [15].

Titanium suffers relatively low SEE loss [13]. In fact, a slight rise is observed at ~10^{19} protons/cm^2 dose. At CERN, Ti foil SEM's have been prepared, baked under vacuum in the lab, then installed in the various transfer and secondary beamlines around the SPS. No subsequent care about exposure to air has been taken [16].

Furthermore, as we discuss in a separate note [17], foil SEM's have an additional advantage of maintaining their tension. Wire SEM's, because of their low ratio of surface area to volume of wire, end up experiencing much heating in the beam: the *dE/dx* deposited by beam particles is proportional to the wire volume and causes a temperature rise of the material. Cooling of the SEM in vacuum, accomplished largely via blackbody radiation, is less efficiently accomplished for a wire because of its relatively small surface area as compared to a foil. As we demonstrate in [17], a wire SEM will elongate due to beam heating and, in most cases, lose all or most of the applied tension on the wires. A foil, in contrast, is able to maintain its tension.

Carbon foil or wire also is a promising SEM candidate material [18]. Its signal yield is constant to 1% after a year exposure to the Los Alamos LAMPF beam. Further, it will not lose more than 1% of its tension when it is strung as a wire plane of 33μm Ø wires [17]. The favorable tension loss is due to its low *Z* (hence low beam heating), it high emissivity (hence efficient cooling), its large heat capacity and low coefficient of thermal expansion. We have procured some 33μm Ø carbon monofilament and experimented with stretching wires on a frame. We found that the carbon filament has a favorable modulus of elasticity of 4.2 g/mm, and a reasonable ultimate tensile strength of 45g (both for 33μm Ø). However, the fiber is extremely fragile against transverse stresses (pressing on the middle of the wire once it is already on the frame, for example). In handling, it is rather like a glass fiber: strong longitudinally, but weak transversely. A prominent concern for such a material is that the wires could break if the accelerator vacuum chamber is ever let up to atmospheric pressure, sending a pressure wave down the pipe. At present, the carbon wires are a backup choice.

IV PROTOTYPE DESIGN

Figures 2, 3, and 4 show schematic assembly views of the prototype SEM developed for the test in the MiniBoone beamline.

Figures 3 and 4 show a beam's eye view of the SEM interior with the foils in and out of the beam, respectively. The foils are stretched over a paddle at ±45º angles. The paddle is large enough to wrap around the beam even when the foils are retracted to the 'out' position. Thus, foil insertion/removal from the beam may be accomplished without interrupting beam operations. With the foils to the out position, the foils cross the 4" aperture of the accelerator pipe, but the frame maintains 4.125" aperture. A full 4" aperture may be achieved with longer travel on the paddle. The paddle slides on two precision 3/8" Ø shafts located inside the vacuum chamber. Four bushings made of PEEK plastic are mounted to the paddle and the bushings slide over the precision shafts. Thus, no lubricated moving parts are located inside the vacuum chamber.

The vacuum chamber is a rectangular chamber with an open end to the far right in Figures 3 and 4. This open end has a rectangular flat flange onto which closes a lid. The vacuum seal is accomplished by crushing an annealed soft (alloy 1100 series) Aluminum wire gasket [19]. The lid has bolted to it a large tray which supports the precision round shafts on which the paddle with foils travels. Thus, to repair a SEM requires removing only the lid+tray assembly. The vacuum chamber body need not be removed from the beamline. Also to be attached to the lid is a bellows-sealed linear motion feedthrough which pushes the paddle in and out of the beam. The feedthrough is produced by Huntington Vacuum. For the prototype, a simple manual push-pull model has been chosen. For the final NuMI design, a motorized model will be used.

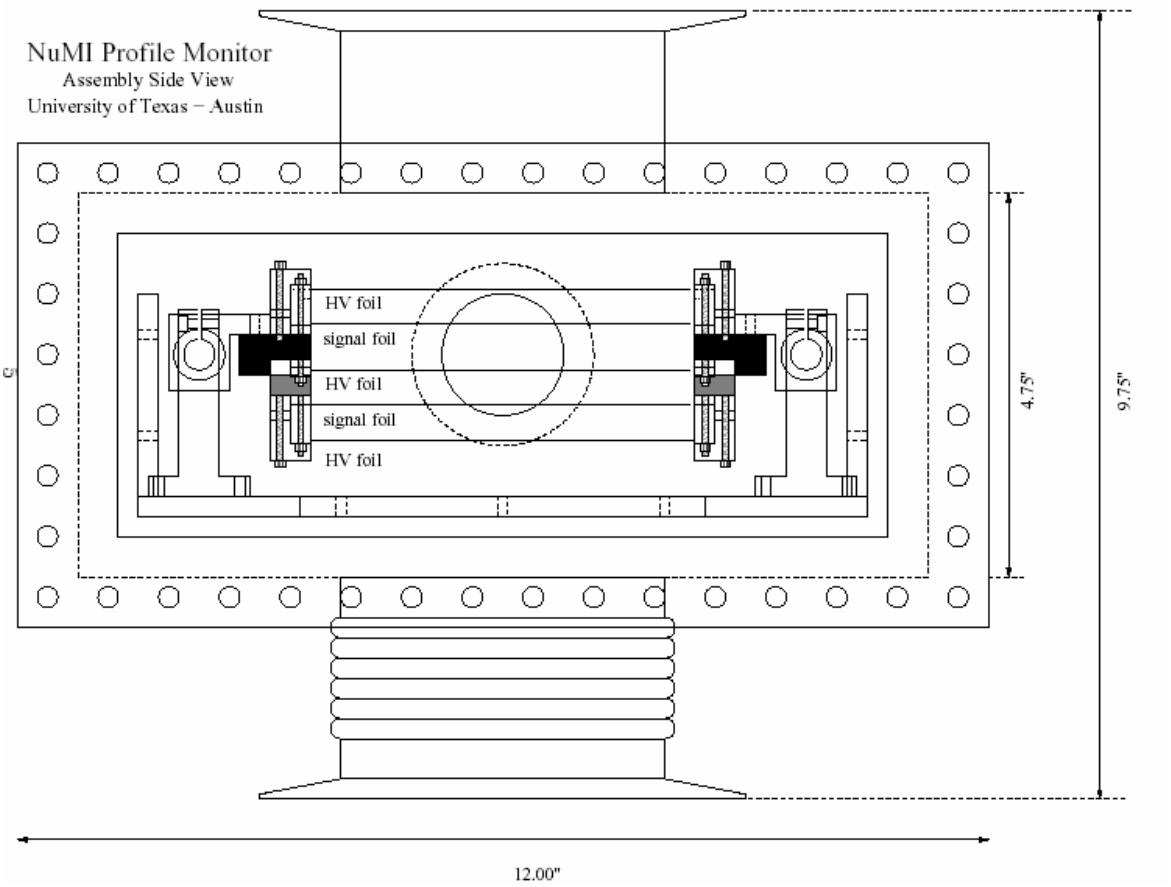

Figure 2: Longitudinal view of the profile monitor SEM. The beam enters the rectangular chamber through the port at the top, passes through the five foils (2 signal and 3 HV foils), and exits out the beam port at the bottom of the figure. This device is inserted in the beam line between other magnets or other components. The lower beam port has a bellows tube to permit loose installation alignment tolerance to the other components in the beamline. The foils are mounted in PEEK dielectric clamps on to an open frame (in black). The frame slides in and out of the beam via rails which run into the page in this view (the rails may be seen to the outside of the frame, and are supported on stands.

Figure 2 is a view of the SEM transverse to the beamline. In this figure, the beam enters the port at the top of the figure and exits at the port on the bottom. The beam passes through 5 foils, 2 signal and 3 HV foils (the latter to draw the secondary electrons from the signal foils efficiently). Visible at the far left and right in Figure 2 are the ends of the two precision shafts along which the paddle slides into and out of the beam. As is indicated in the figure, the five foils are clamped onto the sliding paddle with ceramic clamps. For this prototype, the clamps were fabricated from PEEK plastic.

Not visible in Figure 2 are 12mm Ø holes cut into the HV foils at the location of nominal beam center. These holes permit most of the beam to pass through, thus reducing beam loss in the HV foils. This reduction is important, since the HV foils are solid, as opposed to the segmented signal foils. Obviously, the holes will cause some variation of the clearing field, but the experience reported from CERN is that this variation does not affect secondary electron yield [16]. This is plausible, since the nominal clearing field can be raised to >100V, while the secondary electrons have 20-50 eV energy leaving the foil.

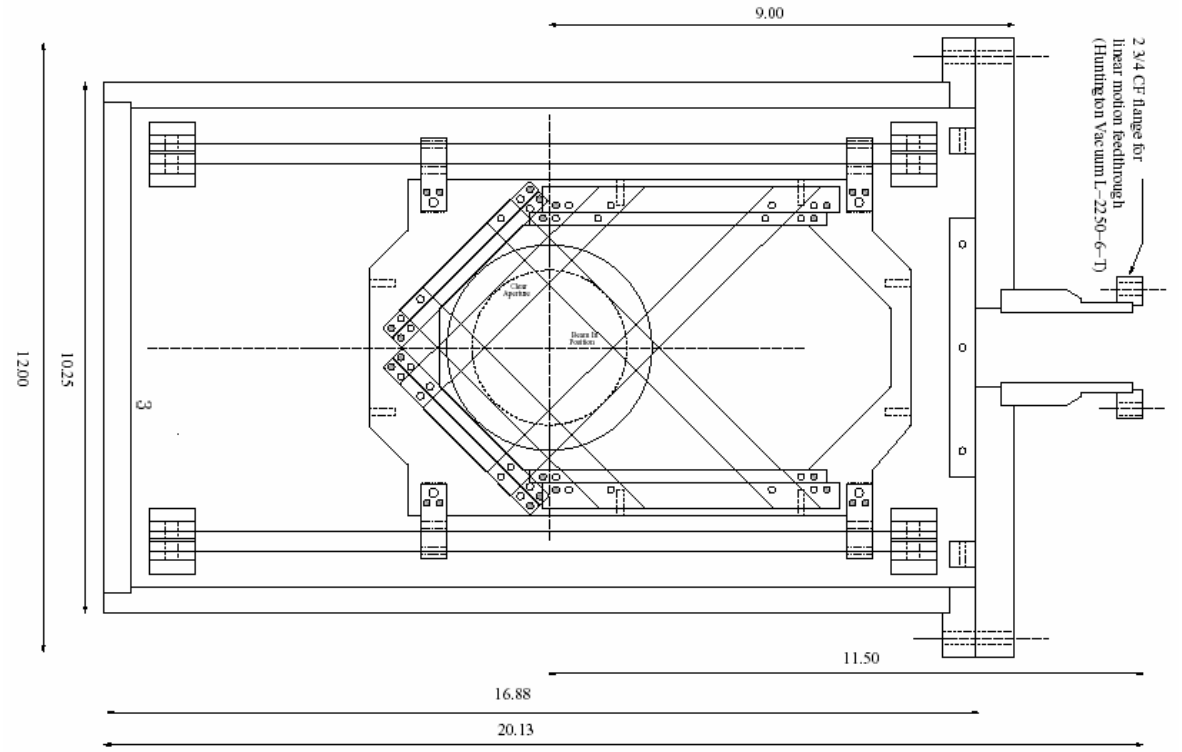

Figure 3: Transverse (beam's eye) view of the interior of the profile monitor. The segmented *U* and *V* foils are stretched over a frame which wraps around the full beam aperture. The frame slides on two precision rails inside the vacuum chamber. In this view the foils are moved into the beam.

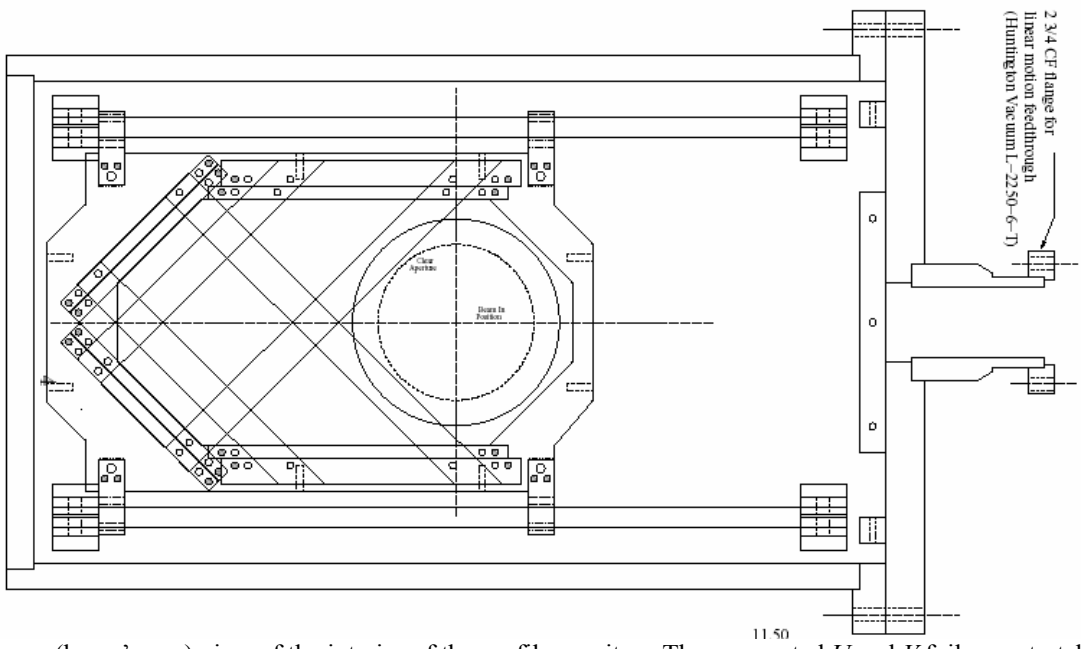

Figure 4: Transverse (beam's eye) view of the interior of the profile monitor. The segmented *U* and *V* foils are stretched over a frame which wraps around the full beam aperture. The frame slides on two precision rails inside the vacuum chamber. In this view the foils are moved out of the beam.

V. FOIL PROCUREMENT

We have purchased a roll of 100 ft. of 5μm Ti foil, 4" width, from Arnold Engineering in Illinois. This vendor was 20% cheaper ($35/lineal foot) than the nearest competitor, and 50%cheaper than the well-known vendor of precision foils, Goodfellow (UK), used by CERN [16]. The thickness variation of the procured foil is claimed to be <10%, but we have not had the ability to measure this. Furthermore, the number of pinhole defects has been quite small. We have thrown away less than 1 foot of the roll so far, while we have used more than 30 ft. for the prototyping process.

Early it was decided not to use the full 4 inch width of the foil for a SEM, and instead to make a 3" wide SEM. This turned out to have a positive consequence: we can throw away the outer 0.5" on either edge of the roll. This turns out to be crucial because the rolling process, in which the material is pressed down from a greater thickness, appears to cause a non-uniformity in the flatness of the material. While the middle part of the foil appears quite smooth, the exterior edges show signs of tapering or worse of having suffered stretching during the rolling process. Thus, the edges do not lay well on a flat surface. To pull them flat would require greater tension.

Arnold Engineering claims to readily be able to produce 0.0001" = 2.5μm thick foil as well. We have obtained a couple samples of 2.5μm foil from Goodfellow just to check that the handling is not significantly more challenging than the 5μm foil. It appears readily possible to make the final SEM's out of the thinner material, which further reduces beam loss, heating in the beam, *etc*.

VI. FOIL TENSIONING

As we note in Ref [17], the effect of beam heating causes elongation of the foil SEM over time. For 5μm thick foil 0.2mm in width, we estimated that the NuMI beam (4×10^{13} protons/spill, 1mm spot size, 8.6μs spill length) will result in a 60μm elongation, with subsequent contraction between spills of order 10μm. Furthermore, the heating expansion is different across the surface of the SEM, with the strips near beam center experiencing the greatest expansion. Previous workers [20] making wire SEM's have actually gone to the effort of installing individual springs on each wire to maintain tension on the wire during beam operation.

With foil SEM's however, a simpler solution exists. CERN employs an accordion-like spring which is impressed into the foil before installing the foil onto a frame [16]. This accordion is extended prior to installing the foil on the frame, which both applies tension to the strips to minimize gravitational sag and also provides the tension for the accordion to contract again when the center of the foil heats during beam operation. A schematic drawing of the accordion spring is shown in Figure 5.

In our experience, the accordion spring also has two other key roles in the fabrication and assembly of the SEM device. First, the Ti foil, as mentioned, is readily stretched inelastically due to handling or due to the initial rolling process which presses a thicker foil down to the 2-5μm final thickness. Such stretching means that the foil does not lay flat, and merely pulling on the ends of a foil does not remove such wrinkles. The accordion spring, however, applies tension to each individual strip, so that if one happens to be stretched longer than its neighbors, then the spring will contract to keep it straight.

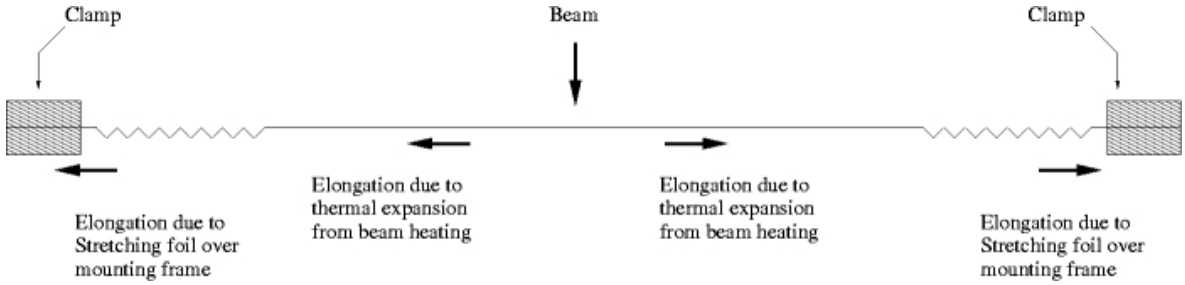

Figure 5: Schematic view of an accordion spring crimped into a foil SEM. Energy deposited into the foil by the traversing beam particles causes linear expansion of the foil strips. If rigidly clamped into a frame, the strips then lose tension. The accordion spring, stretched beyond its relaxed length when the foil is mounted on the frame, contracts when the central part of the foil expands, thus applying continued tension

Second, the accordion spring provides some safety during the eventual bakeout of the SEM vacuum chamber: to drive away water vapor and achieve 10^{-8} Torr final pressure, the SEM must be baked at elevated temperature while it is pumped, and the different coefficients of thermal expansion of different materials can result in the tearing of a foil mounted on a frame when the entire SEM is heated. The springs thankfully allow the frame to expand differentially with respect to the foil.

We developed a jig to press accordion-like springs into the two ends of our foils. The jig consists of a machined plate with Vee grooves over which the foil rests. Tapered blades are pressed into the Vee's to 'coin' the metal. The blades have been sanded with tissue to smooth the tips and avoid shearing of the foil. The blades, of course, must be pressed sequentially to permit the foil material to advance into the jig. In Figure 6, we show a small foil sample that has been crimped. The accordion "vee's" are 1mm wide, and 8 vee's have been crimped per side of the foil. The figure shows the effect of stretching the accordions by 50%.

Figure 7 shows the results of measurements of the spring tension in the accordion springs. In these measurements, the foil of Figure 6 was suspended vertically from one end. The lower end hung freely, and successively more weight was taped to the lower edge of the foil. The position of the foil was observed using a Wild Heerbrugg N2 optical telescope. The foil width is 3", and the foil in this test has a total of 15 "vee's" crimped into it. As can be seen, a spring constant of 45g/1.75mm = 26g/mm may be inferred from the linear portion of the graph. The maximum elongation for linear expansion is apparently ~2mm for 15 accordion "vee's". For our final prototype SEM, we crimped 24 accordions into the foil, so we expect a maximum allowed elongation of 3mm. Given that the foil tested here is 3"=76mm in width, we expect that the 1mm wide strips in the prototype SEM will have an applied tension of (26g/mm) × (3mm) × (1mm/76mm) = 1.1 g.

Furthermore, we have tested a foil crimped in a frame at temperatures of up to 150ºC. No additional sagging has been observed after the temperature has been cycled several times. Thus, the crimp does not appear to relax.

The tension in a single strip of 1.1g is actually less than what could be applied in the foil if it is simply tensioned over a frame, like on a snare drum head. The advantage of the spring concept is that the tensioning is elastic and does not damage the material. Thus, beam heating should always be compensated correctly.

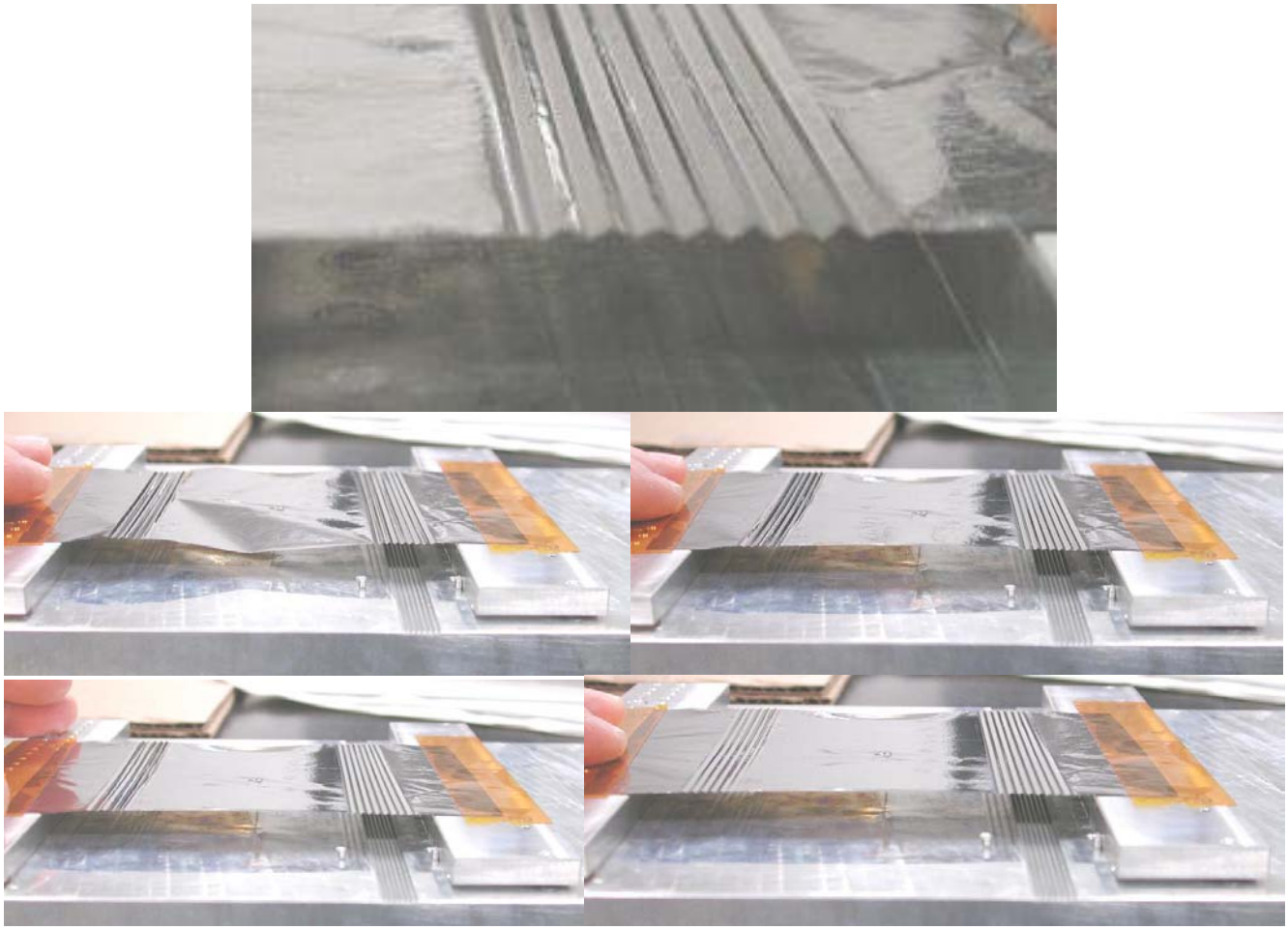

Figure 6: Test crimp of a pair of accordion springs into the Ti foil. Each accordion consists of eight 90º "Vee's", which may be extended to greater than 120º to apply tension in the foil. Above is a close-up view of the accordion. Below are 4 views of an increasingly-tensioned foil.

There are two concerns brought about by the limited tension per strip. The first is the gravitational sag, which will be greater than for a conventional wire chamber strung at ~90g. The second is the electrostatic stability, given that the signal foil will be positioned between two high voltage foils which collect the emitted electrons.

Regarding electrostatic stability, the condition for electrostatic stability for a wire chamber of length L and wire spacing s with wire tension T (in g) and voltage V is [21]:

$$\frac{s}{L} \geq 1.5 \times 10^{-3} V(\mathrm{kV}) \sqrt{\frac{20\ \mathrm{g}}{T}}\ ,$$

which we can invert to determine the maximum length on a wire given spacing s=1mm. We assume T=1.1g, and V=0.2kV, to obtain a length bound of L<780mm, or L<31". For a spacing of 0.5mm, as will be used in the two target SEM's, the maximum strip length can be 15". Our prototype design has a maximum strip length of 7.5". It should be noted that the CERN experience suggests no more than 50V will be required for the HV foils as long as a positive beam is being measured (to be contrasted with CERN's e^- beams from LEP which require >800V bias on the SEM [22]).

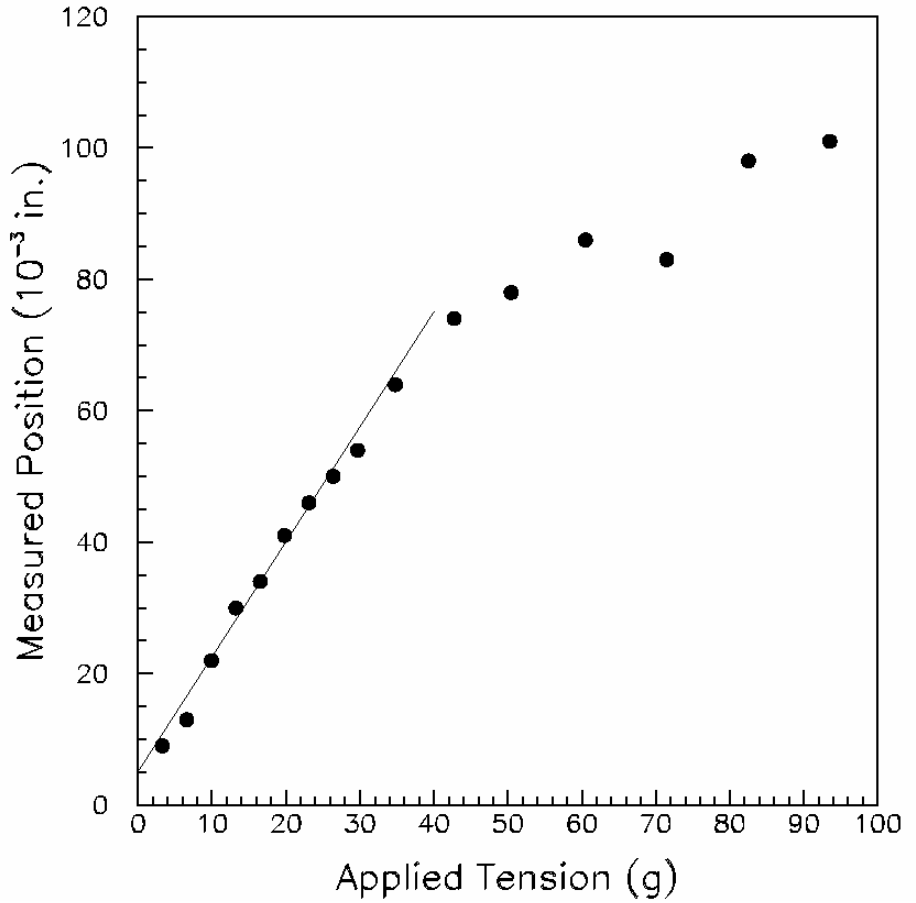

Figure 7: Measured stretching of a 3" wide foil suspended from one end on a frame and on the other end of which were hung small weights. The position of the freely-moving end was measured using an optical telescope.

As for mechanical sag, the sag δy of a limp string of cross-sectional area A, length L, density ρ, may be approximated as

$$\delta y = g\rho AL^2/T$$

The titanium strips are not necessarily a limp string, but the approximation should at least serve for an order of magnitude. This expression gives, for L=7", a tension T=1.1g, the density of Titanium ρ=4.5g/cm^3, and a 5μm×0.2mm strip, a sag estimate of δy = 0.1mm.

Finally, we note that the additional sag caused by beam heating will not be problematic. As discussed in Ref [17], the expansion due to beam heating is 60μm. This is 0.06mm/3mm = 2% of the total elongation applied to the foils when they are tensioned on the frame. Thus, we expect to lose only 2% of the tension, and thus gain 2% more gravitational sag.

VII. Foil Machining

The Ti foil must be slotted with 45 parallel slots. For the final NuMI foil design, the slots will vary from 0.010" in width near the edges and grow to 0.030" in width so as to achieve a narrow strip near beam center. We have explored cutting of the Ti foils with several vendors. One failed attempt would have utilized laser machining, but the laser caused excess heating of the material. Two vendors attempted chemical machining with hydrochloric acid. A successful example of such a foil, produced by Vaga Industries in California, is shown in Figure 8. The strips have narrower dimension over the spread of the 3" beam aperture. Halo foils of 0.62" dimension are also etched as part of the process. The strips are quite sharply defined when viewed under a microscope.

Figure 9 shows one of the foils to be used for the prototype SEM being assembled for the MiniBoone test. This foil differs from the NuMI design in that it does not have the narrower span of strips near the beam center. Eliminating this feature has allowed us to make more rapid progress on tooling and handling of the foil without too many complications and delays. The vendor experienced difficulty delivering foils of the thinner variety without any imperfections. The imperfections were mainly strips that had been stressed during their cleaning process by mechanical wiping of the piece. These stretched strips do not lie very flat when the piece is placed on a flat surface, and would require much additional tensioning of the accordion springs to straighten out. Now that the "hands-free" acid cleaning process has been refined at UT-Austin, it is likely that the thin strip model can be revisited. Also, the vendor has located and successfully employed another, acqueous-based photoresist which, although still requiring the acid bath, does not require nearly the mechanical handling to remove.

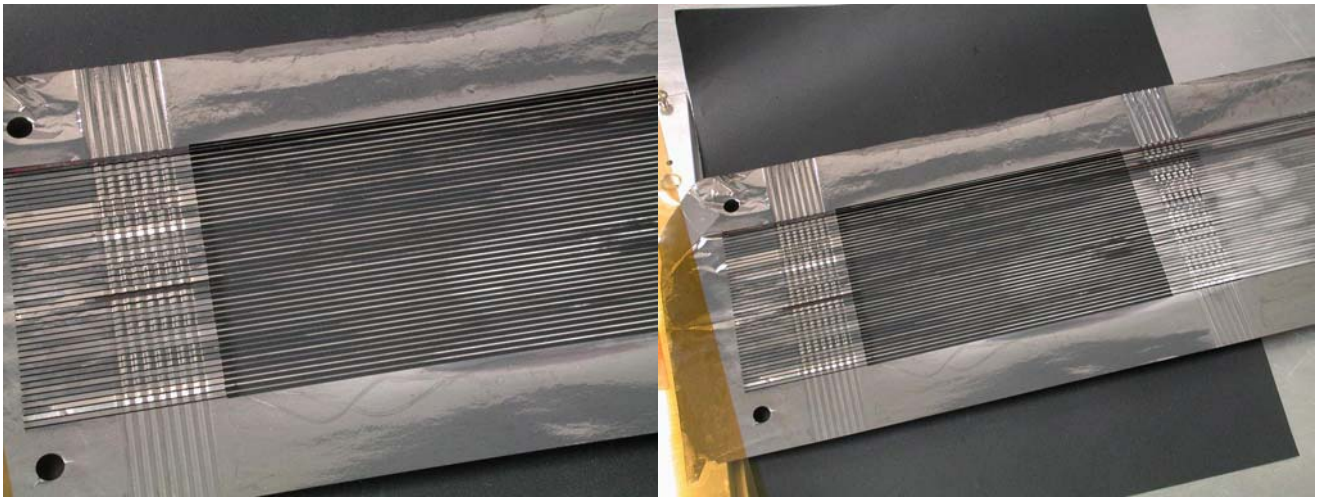

Figure 8: A 5μm Ti foil etched with strips every 1.00mm center-to-center. Each strip is separated from its neighbor by 0.25mm and at its end is 0.75mm in width. Over the 3" beam aperture, the strips are reduced to 0.25mm in width so as to reduce beam losses in the strips. The accordions are pressed into the 0.75mm wide parts of the strips.

Figure 9: One of the signal foils for the prototype SEM prior to acid cleaning. (left) View near one of the ends of the foil, showing the accordions already pressed into the strips. The evidence for photoresistive layer yet remaining on the foil is the fact that several strips are adhered together (*eg*. the 2nd and 3rd strips from the left). (right) View of the foil in the acid bath, showing photoresist (in yellow) near the edge of the halo strip which is to be cleaned by the acid.

VIII. FOIL CLEANING

After the foil has been chemically machined, it is rather stained and discolored. The discoloration is leftover photo-resistive layer from the lithography process to etch the strips. This photo-resist is quite durable, since it must survive in a hydrochoric acid bath to etch the Ti foil. For a SEM, such surface layers would cause signal degradation after prolonged beam exposure.

Several solvents such as toluene, xylene, and several acids have been attempted. Undiluted sulfuric acid has been observed to be an effective solvent for the photoresist (see Figure 10). The complication, of course, is that washing away the acid with water induces a tremendous exothermic reaction. The temperature can exceed 100ºC. In fact, during our first attempts to clean away the acid, the foil was blackened and shriveled by the heat. In subsequent attempts, even supporting the foil on a stainless steel substrate was sufficient to trap the viscous acid beneath the foil. This trapped acid could cause local heating of the foil and holes in the material. Thus, we subsequently developed a frame for submersing the foil in the acid freely and then maximally exposing it to the H_2O wash.

Figure 10: (left) Bathing of the Ti foil in undiluted sulfuric acid to remove the residual photoresist layer. (right) The sulfuric acid after foil cleaning.

IX. FOIL MOUNTING

The next few pages demonstrate the procedures developed for suspending the foils on clamps and mounting these clamps onto the aluminum frame.

The procedures to mount these foils are substantial, or at the very least outside the recent realm of experience at FNAL, where considerably more expertise in wire-stringing exists. As part of the development of the SEM prototype, we have built several jigs to permit "hands-free" manipulation of the foils. This reduces the risk of stretching one of the strips during the handling.

It should be noted that one important study had not been performed for this prototype: the definition of "how much tension must be applied". In this assembly, a 'reasonably large' tension was applied by crimping 8 accordions on one end and 16 on the other end of the foil, and stretching these accordions to the point where they are nearly flat. At this tension, the foils appear to be quite planar and many imperfections or wrinkles in the foil are 'pulled straight.' Even at this tension, however, the foils readily flap around if one blows gently on them. The results of Section VI indicate that our accordions were likely overstretched for this prototype. A more rigorous program of exploring how many accordions can be accommodated, how much tension induced, and how flappy the strips will ultimately be, must be undertaken in the future. Our bias for this prototype was driven by a calculation that indicates that the heating expected in the MiniBoone beamline will be negligible (<100ºC) [17], so it would be better to overtension the foils than undertension them.

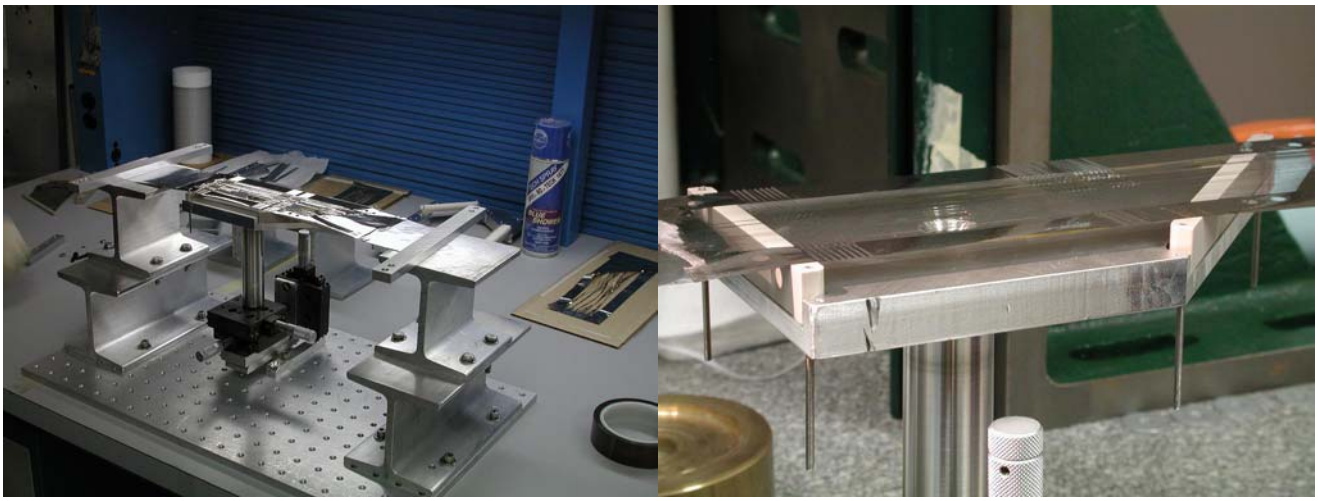

Figure 11: Jig used to mount a signal foil on its combs/clamps. The signal foil is tensioned over two I-beams, while a 3-axis set of linear motion slides brings a jig holding the combs into place under the foil. The combs pictured here are made of PEEK, although the eventual combs will be made of ceramic. Epo-Tek H27D conductive epoxy was applied to each of the 44 grooves of the PEEK into which a strip slides, anchoring each strip at its two ends. Thus, when these two combs are transferred into the final frame which holds the SEM, the position is defined by the combs and the tension by the epoxy.

Figure 12: (left) Curing of the epoxy under 150ºC for 1 hour. (right) The signal foil after the PEEK combs have been glued beneath the foil. At this point a distinct error in the clamp was noticed: the clamp "teeth" should have been 0.0141" in width and the grooves 0.0425" in width, when viewed at a 45º angle, in order to permit the 0.030" wide strips to maintain their 0.040" center-to-center spacing. These combs, however, were machined with 0.014" teeth and 0.042" wide grooves, leading to an overall stack-up error of nearly 0.025" across the whole span of the foil. The error in the dimension lead to a 'gathering' of the foil toward this end of the foil shown, hence the different strips catch the light differently.

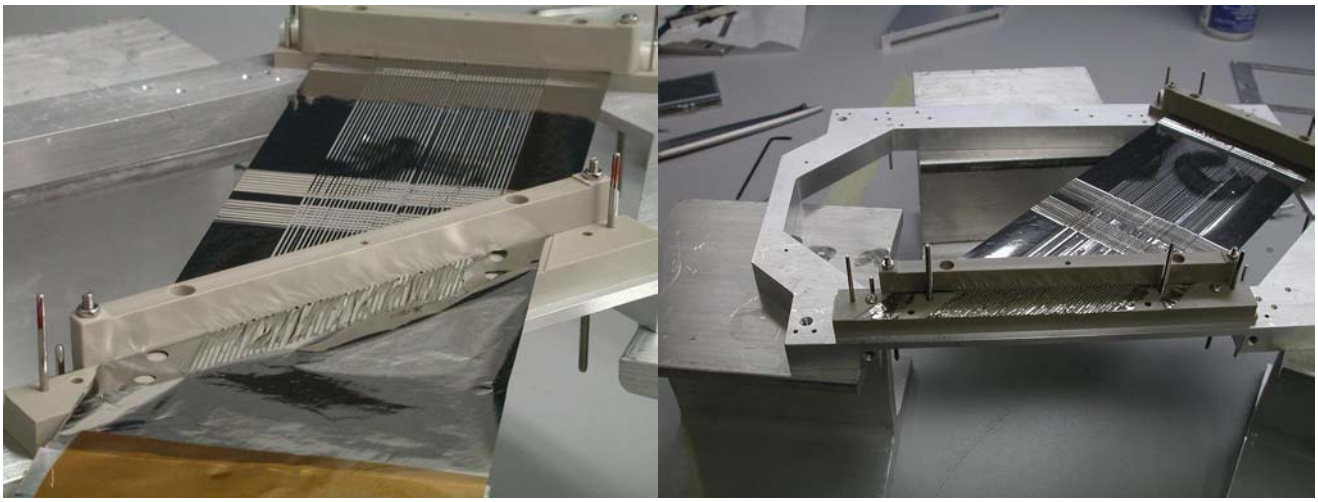

Figure 13: (left) Transfer of the signal foil into the SEM frame. The PEEK combs are inverted by the jig two which they were bolted, and the threaded rods holding them are threaded into the frame so that the frame now captures them. The foil, furthermore, is made to pass over the top of another comb at a different height, so as to again constrain it and hold its tension. (right) The signal foil after the excess material has been cut away. The strip ends are laying in the grooves of an additional comb in which the signal cables will later be epoxied.

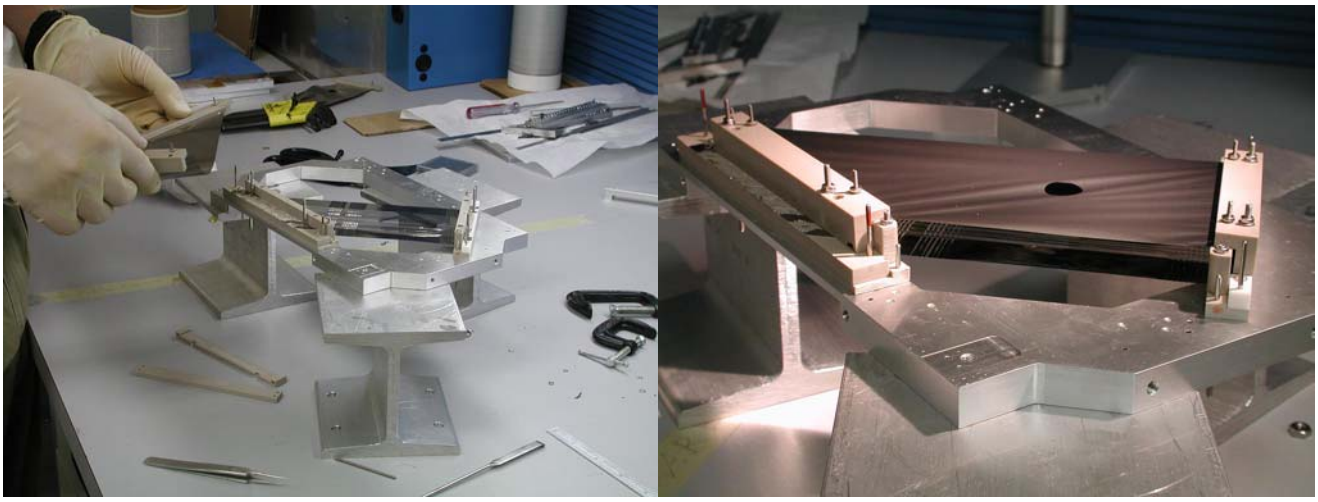

Figure 14: (left) The signal foil in the SEM frame, with the upper HV foil about to be installed. (right) The HV foil now installed so that it hovers 0.5" above the signal foil. A total of 3 HV foils will eventually sandwich the *X* and *Y* signal foils. Note that the HV foils have the same 3" width as the signal foils and also have a 12mm hole where beam center is expected. The experience from CERN is that a 12mm hole reduces beam loss and may be accommodated with 'no loss of signal' if the HV foil is at least 12mm from the signal foil. Clearly, this assertion must be tested.

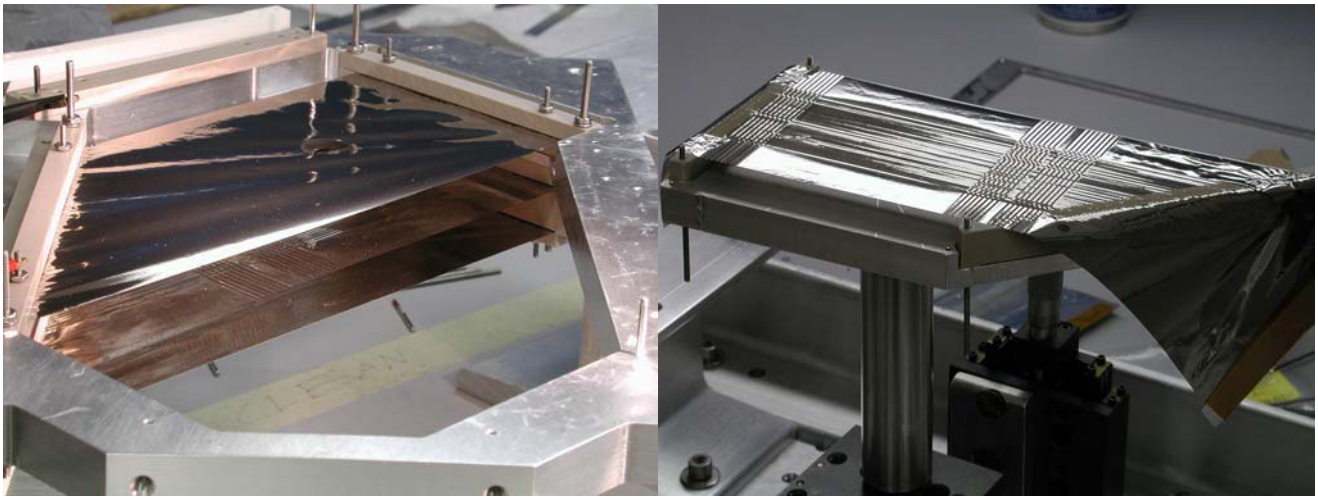

Figure 15: (left) The SEM frame is now flipped over and the 'middle' HV foil is inserted. This HV foil lays between the two signal foils. (right) Readying the second signal foil for mounting on the SEM frame. Here it has been epoxied to its combs on the adjustment and tensioning jig.

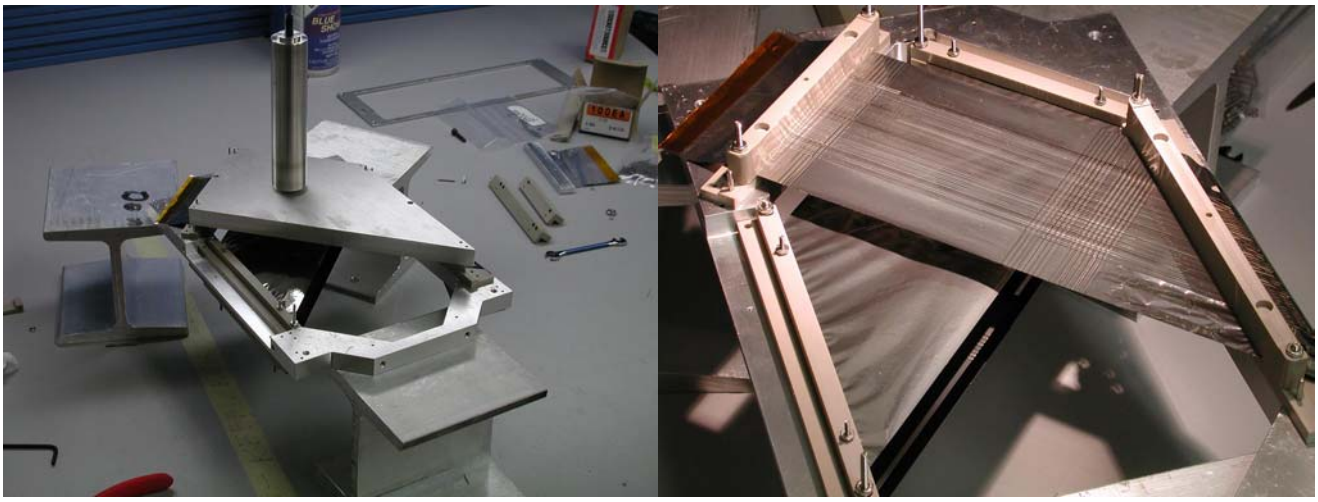

Figure 16: Transfer of the second signal foil into the SEM frame. (left) The PEEK combs are inverted by the jig to which they were bolted, and the threaded rods holding them are threaded into the frame so that the frame now captures them. (right) The jig is removed once the anchoring of the combs has been transferred from it to the SEM frame. At this moment two signal and two HV foils are in place on the SEM frame.

Figure 17: View of the SEM frame before installation of the last HV foil. Inspection of the photo at left will show a 'cross-hatched' pattern of both the *X* and *Y* view foils being visible through the backlit hole of the HV foil. At right, note that the accordions have been pressed into the signal foil so that they are confined to the space outside the beam aperture of 3" (the region crossed by the middle HV foil which is 3" in width). Note that additional accordions could be crimped into the longer strips, which would have the benefit of giving greater tension to the longest strips. The tension appears to increase as the number of accordions grows, but does not depend on the size of the accordions (all the spring action in the crimped/creased vee of an accordion).

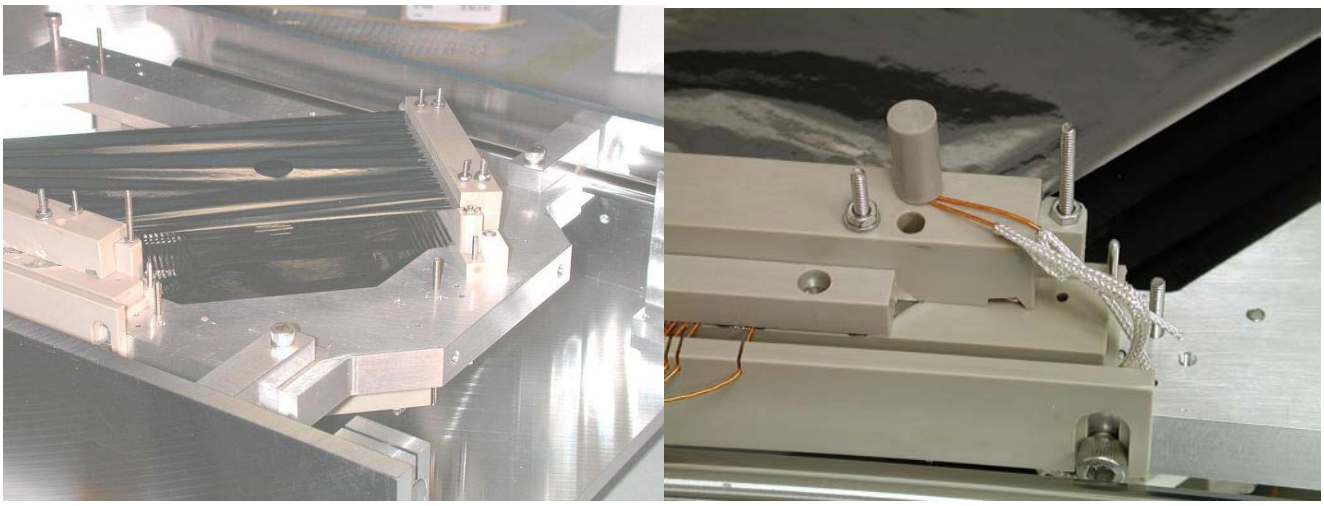

Figure 18: (left) View of the SEM frame after installation of the last HV foil. As before, note the 12mm diameter hole in the HV foil for the beam to nominally pass through with reduced interactions. (right) The HV connection to the foil is made via a shielded kapton cable which is soldered to a 0-80 screw which protrudes through the foil (the smaller screws closer to beam center in the left photo). The 0-80 screw is subsequently concealed under a PEEK threaded cap to prevent discharge to grounded screws and also the vacuum can. All the HV foils are daisy-chained together.

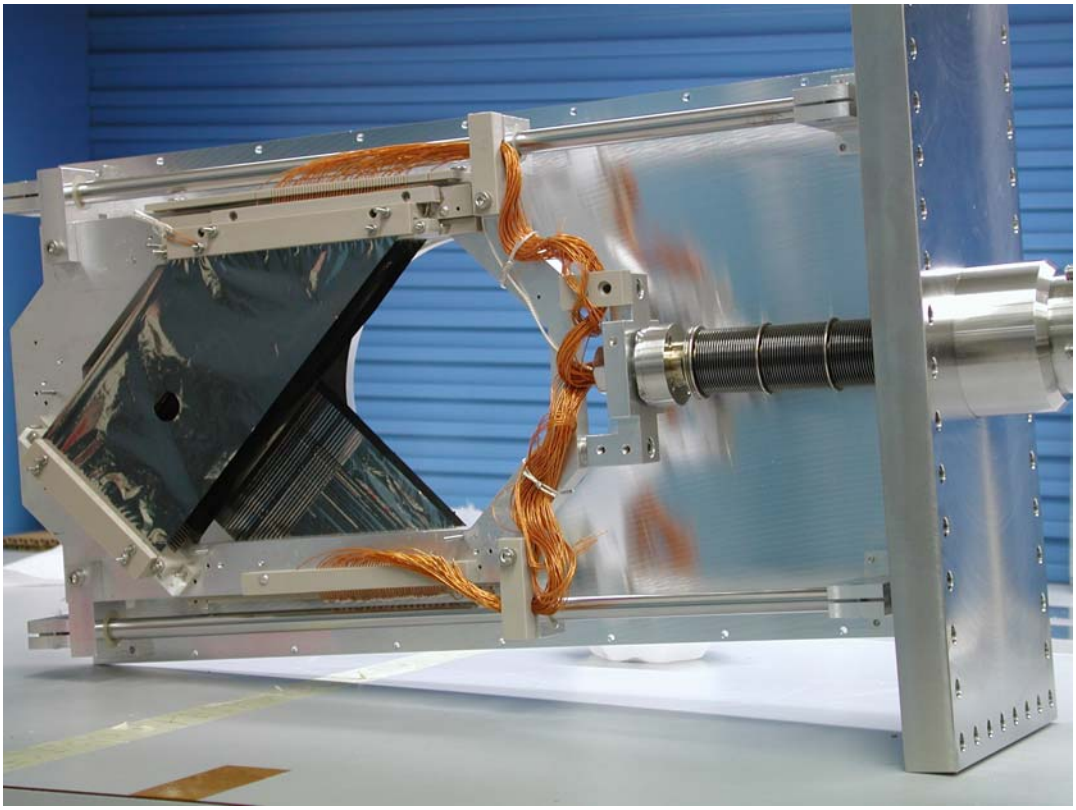

Figure 19: The SEM frame now resting on its rails which are supported by 4 stands in a "U" channel tray. This tray is bolted to the inside of the lid to the vacuum chamber. The linear motion bellows feedthrough protrudes through this lid and conducts the kapton signal cables through its hollow shaft to the exterior of the can. At the exterior (air) side of the feedthrough is mounted a box with signal connectors and an HV connector. The cables pass through the hollow shaft of the motion feedthrough into this box, and cables are soldered to pins on the inside of the feedthrough box.

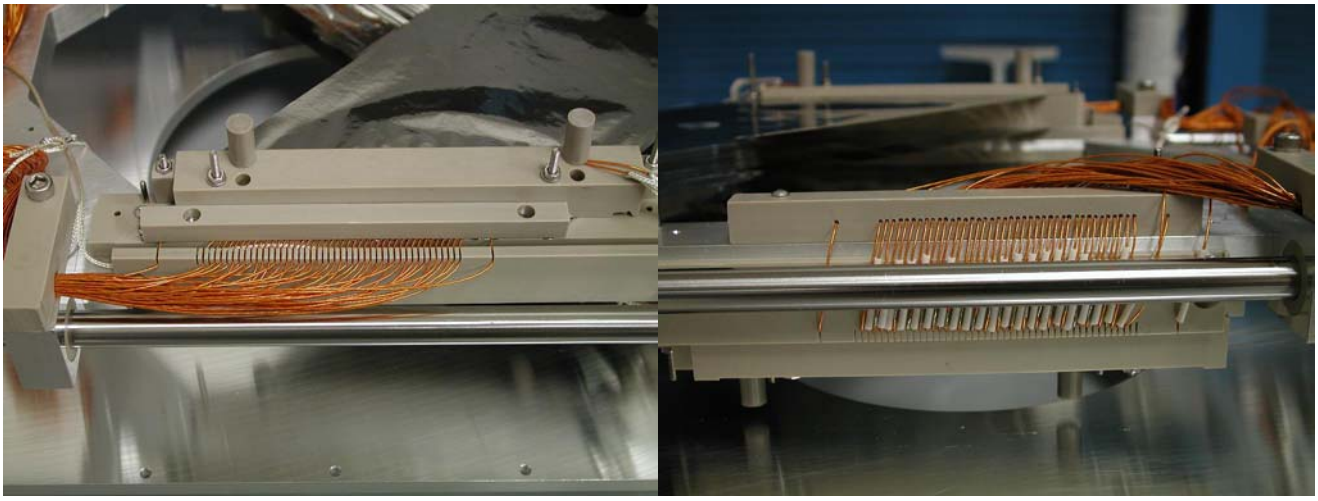

Figure 20: Expoxied connections of foil strips to unshielded kapton signal cable (0.020" OD, conductor 0.010" Ø). Each strip and its kapton cable rest in a 0.010" deep groove in the PEEK clamp. (left) Detail of the upper foil connection in Figure 19. (right) Detail of the lower foil connection in Figure 19.

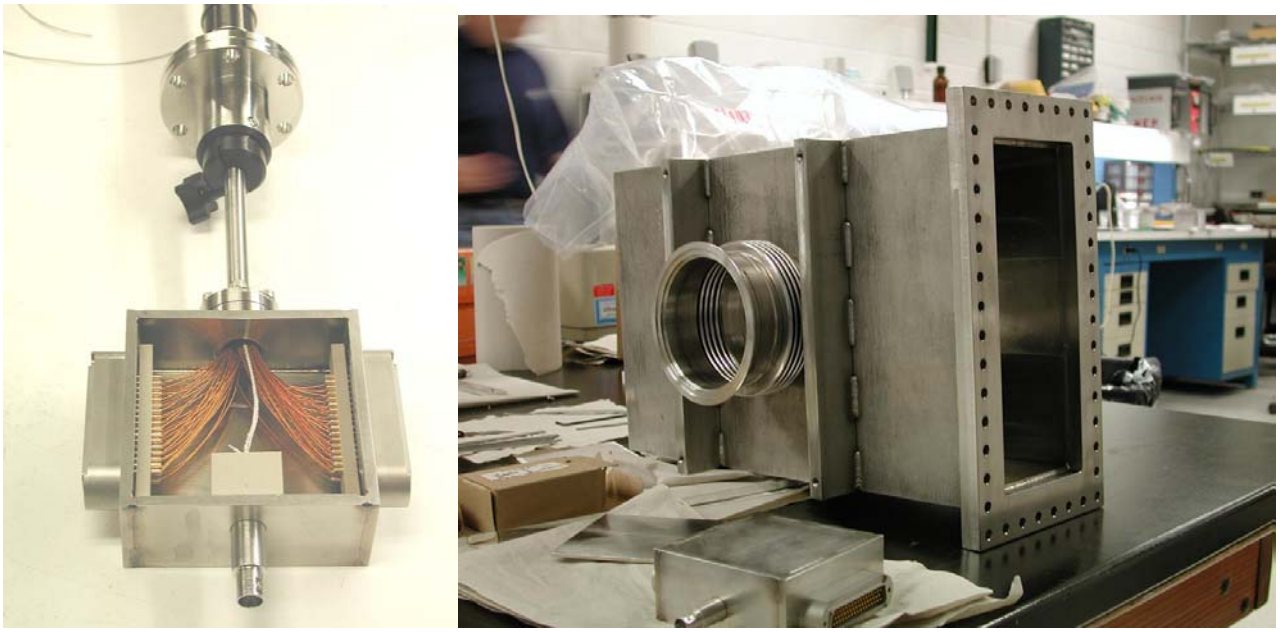

Figure 21: (left) Closeup view of the feedthrough box before it was welded shut. The 50-pin connectors are fabricated by Ceramaseal, Inc., and are ceramic-insulated. The SHV connector will be attached to all 3 HV foils. It too is ceramic insulated. All connectors are bakeable to 350ºC, far above the recommended point for the SEM. (right) The vacuum can for the SEM. The beam passes through the 4" diameter port on the left front face and out a similar port to the rear. The KF at front is welded to a bellows. The opening to the far right face of the can accepts the lid assembly shown in Figure 19. Hence, replacement of a failed SEM principally requires only disconnecting the lid, pulling out the tray, and replacing the tray assembly and lid with a new one.

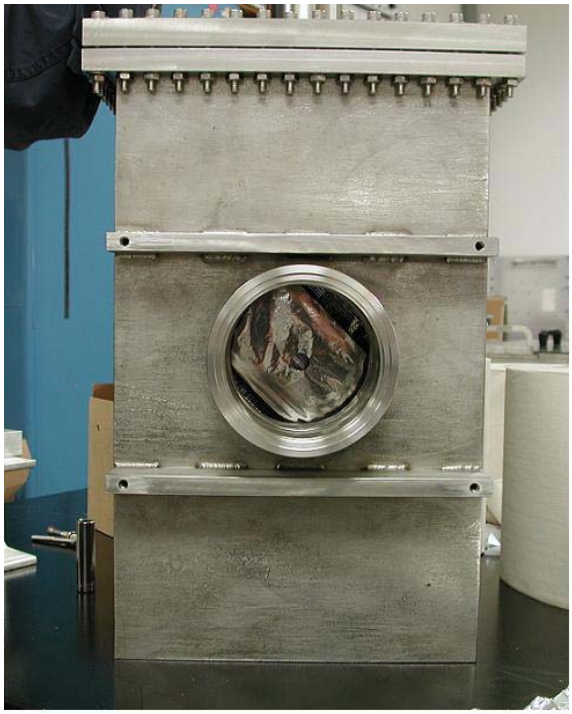

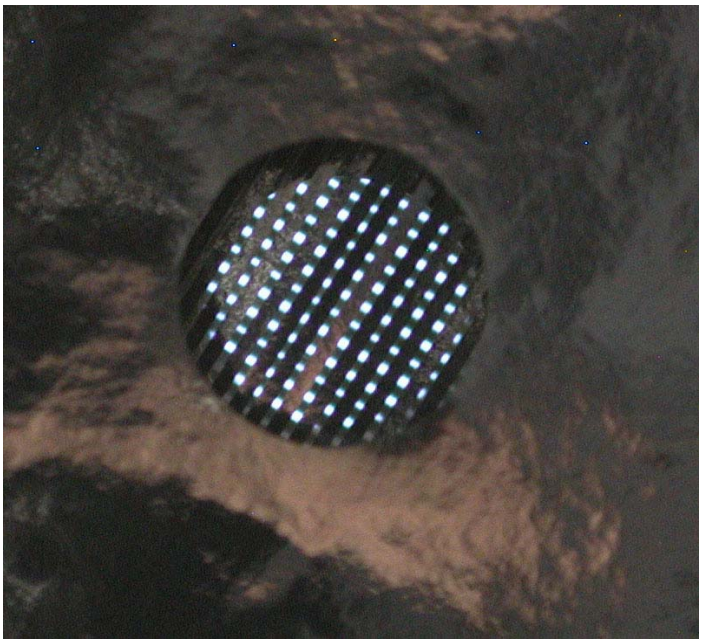

Figure 22: (left) Fully-assembled SEM inside its vacuum canister. (right) Close-up view of foils through the beam port. Both the *X* and *Y* foils are visible through the hole in the HV foil.

X. CONCLUSIONS

We have developed a prototype SEM for NuMI that will be tested in the MiniBoone line this summer. Already, the assembly of the device has indicated some changes that should be made for future models:

1. The feedthrough signal and HV connectors should no longer be located in a box at the end of the motion shaft, but instead in the vacuum lid; the cables then will simply have to retract when the paddle moves. This connector box is slow to pump out.
2. The circular PEEK bushings on which the paddle slides should be replaced with V- or C-shaped bushings, and the bushings should be made of Vespel, a higher temperature plastic. In our prototype, the PEEK seized on the shafts after several temperature cycles.
3. Survey markers should be added to the vacuum lid and to the PEEK/ceramic clamp which mount the foils. Our prototype did not require accurate survey, but attempts to locate the foils were difficult without markers.
4. The signal lines should be crimped to the feedthrough pins to reduce the number of solder joints inside the chamber. As the PEEK clamps are switched to ceramic and the PEEK bushings to Vespel, the solder joints will actually be the major temperature limitation to higher temperature baking. For the prototype, we were limited to 125º-150ºC bakeout, which required ~ 1week. The temperature limitation will be the Epo-Tek epoxy, which must be exposed to <350ºC.

A second prototype is being constructed with these design changes.

ACKNOWLEDGEMENTS

We are very grateful to Gianfranco Ferioli of CERN for sharing his SEM design ideas with us and for his extensive advice throughout this project. We are also indebted to our Fermilab colleagues for their critical and constructive comments at the reviews conducted of this prototype system, in particular Rick Ford, Dave Pushka, Gianni Tassotto, and Bob Webber. Sam Childress, Rick Ford, Gianni Tassotto, and Bob Zwaska did a great deal to make the MiniBoone test possible, including obtaining permission for the test, setting up cable runs, performing the bakeout and residual gas analysis of the chamber, and building an instrument stand for the test location. Thanks to Sam Childress and Bruce Baller are due for support of this project.

REFERENCES

[1] H. Bruining, Physics and Applications of Secondary Electron Emission, (London: Pergammon Press), 1954.
[2] G.W. Tautfest and H. R. Fechter, *Rev. Sci. Instr.* **26**, 229 (1955).
[3] E.J. Sternglass, *Phys. Rev.* **108**, 1 (1957)
[4] B. Planskoy, *Nucl. Instr. Meth.* **24**, 172 (1963).
[5] D. Harting, J.C. Kluyver and A. Kusumegi, CERN 60-17 (1960).
[6] J.A. Blankenburg *Nucl. Instr. Meth.* **39**, 303 (1966).
[7] R. Anne *et al.*, *Nucl. Instr. Meth.* **152** 395 (1978).
[8] See, for example, the study by L. N. Hand, Fermilab Technical Memo TM-385 (1972)
[9] S.I. Taimuty and B.S. Deaver, *Rev. Sci. Instr.* **32**, 1098 (1961)
[10] D.B. Isabelle and P.H. Roy, *Nucl.Instr. Meth.* **20**, 17-20 (1963).
[11] E.L. Garwin and N. Dean, "Method of Stabilizing High Current Secondary Emission Monitors," in *Proc. Symp. on Beam Intensity Measurement*, Daresbury, England, p 22-26, April 1968.
[12] V. Agoritsas and R.L. Witkover, *IEEE Trans. Nucl. Sci.* **26**, 3355 (1979).
[13] G. Ferioli and R. Jung, CERN-SL-97-71(BI), published in *Proceedings of Beam Diagnostics and Instrumentation for Particle Accelerators* (DIPAC), Frascati (Rome), Italy, Oct. 12-14, 1997.
[14] R. Drucker, R. Ford, and G. Tassotto, FERMILAB-Conf-98/062, published in *Proceedings of Beam Diagnostics and Instrumentation for Particle Accelerators* (DIPAC), Frascati (Rome), Italy, Oct. 12-14, 1997.
[15] R. Ford, FNAL, private communication.
[16] G. Ferioli, private communication.
[17] T. Osiecki and S. Kopp, "Studies of Beam Heating of NuMI Proton Beam Profile Monitors," NuMI-B-926 (2003).
[18] D. G. Gilpatrick, Los Alamos National Labs, private communication.
[19] A. Erwin, "An Annealed Aluminum Wire Gasket as a Radiation Hard Seal for Beam Monitoring Chambers," NuMI-B-862 (2002).
[20] J. Krider and C. Hojvat, *Nucl. Instr. Meth.* **A247**, 304 (1986).
[21] K. Hagiwara *et al.* "Review of Particle Properties," *Phys. Rev.* **D66**, 010001 (2002).
[22] J. Camas *et al.*, "Screens *vs*. SEM Grids for Single Pass Measurements in the SPS, LEP, and LHC," CERN-SL-95-62(BI), published in *Proceedings of Beam Diagnostics and Instrumentation for Particle Accelerators* (DIPAC), Lübeck-Travemünde, Germany, 28-31 May, 1995.